J. Plasma Physics (2007), *vol.* 73, *part* 2, *pp.* 241–256.
doi:10.1017/S0022377806004533 First published online 30 May 2006 Printed in the United Kingdom

Interaction of Alfvén front with the plasma anomalous resistance layer

N. MAZUR[1], E. FEDOROV[1], V. PILIPENKO[1] and A. LEONOVICH[2]

[1]Institute of the Physics of the Earth, Moscow 123995, Russia

[2]Institute of the Solar–Terrestrial Physics, Irkutsk 664033, Russia

(Received 27 November 2005 and accepted 4 February 2006)

Abstract. The efficiency of the Alfvén impulse excitation in the auroral zone of the terrestrial magnetosphere upon the onset of the anomalous field-aligned resistance has been estimated. The impulsive disturbance excited during the onset of anomalous field-aligned resistance and electric field may signify the transition of a global magnetospheric instability into the explosive phase with positive feedback. We consider the self-consistent problem on excitation of anomalous resistance at the front of field-aligned current and reverse influence upon it from the induced currents. The analytical solution of the self-consistent problem has shown that during the entrance of field-aligned current front into the anomalous resistivity layer (ARL) an Alfvénic impulse is generated. The interaction of the external current with ARL results in the delay of the current growth. The impulse duration and delay time depend on the ratio between the Alfvén damping scale and external current width. The solution obtained indicates the possibility of using the Alfvénic impulse as an indicator of distant occurrence of anomalous resistance.

1. Introduction

Anomalous resistance due to the high-frequency turbulence is a ubiquitous element of high-temperature collisionless space and laboratory plasmas [1, 2]. The occurrence of the anomalous resistance on the high-latitude field lines is a key element of the magnetosphere–ionosphere interaction in the near-Earth environment [3, 4]. For a long time it was known that the excitation of the anomalous resistance upon propagation of intense field-aligned current disturbances is possible [5–8]. In the region with field-aligned current j_0, the emergence of an anomalous resistive layer with a finite field-aligned conductivity $\sigma_\parallel$ results in the occurrence of anomalous electric field $E_\parallel \simeq j_0/\sigma_\parallel$. This field-aligned $E_\parallel$ accelerates electrons. In the terrestrial magnetosphere, the accelerated electrons cause additional ionization of the ionosphere and activation of the auroral activity. Ionization and relevant modification of the ionospheric conductance is the physical basis of various mechanisms of feedback in the coupled ionosphere–magnetosphere system [9, 10]. This positive feedback instability may eventually lead to the onset of an explosive phase of a substorm.

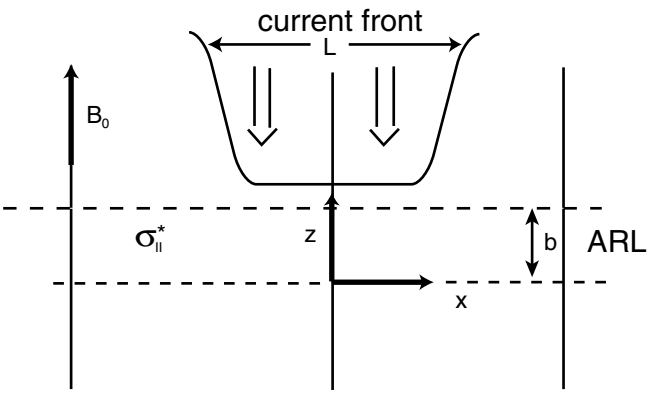

Figure 1. Sketch of the model describing the interaction of an Alfvén front with the ARL.

The intensity of field-aligned currents, transported by a front of Alfvén-type disturbance, may be sufficient for the excitation of anomalous resistance in space plasma. The sudden switch-on of the $\sigma_\parallel$ results in the excitation of an Alfvénic impulse. The possibility of an Alfvénic impulse generation related to the onset of an anomalous resistance on auroral field lines was originally suggested by Arykov and Maltsev [11]. Later on, we developed a mathematical formalism for the description of the impulse spatial structure, discussed some implications of this model, and provided some observational evidence in favor of this hypothesis [12]. Therefore, the occurrence of such an impulse signifies the 'switch-on' of the anomalous resistivity on a field line, even far away from the observation point.

However, the previous models considered the structure of the Alfvén impulse originating after a momentary occurrence of the anomalous resistance. In a realistic situation, the induced currents may influence the total field-aligned current and establishment of anomalous resistance regime. In this paper we consider the self-consistent problem on excitation of both the anomalous resistance and Alfvén impulse at the front of field-aligned current entering the region with favorable conditions for the excitation of plasma turbulence.

2. Model of the resistive layer and basic equations

Here we develop a mathematical formalism for the description of the Alfvén impulse generation during the switch-on of anomalous resistivity in a resistive layer, induced by an external non-steady current. The model is shown schematically in Fig. 1. The homogeneous geomagnetic field is directed vertically upwards, $\mathbf{B}_0 = B_0\hat{\mathbf{z}}$. The homogeneous magnetospheric plasma has a vanishing transverse static conductivity and infinite field-aligned conductivity $\sigma_\parallel = \infty$. In many realistic situations, the threshold for the excitation of the anomalous resistance is lower within a certain region [13] further named as the anomalous resistivity layer (ARL). In the model considered, the finite $\sigma_\parallel$ occurs in the vicinity of the plane $z = 0$ inside a layer with thickness b.

The considered mathematical model is based on the system of Maxwell equations

$$\nabla \times \mathbf{E} = -\frac{1}{c}\partial_t \mathbf{B}, \quad \nabla \times \mathbf{B} = \frac{4\pi}{c}\mathbf{j},$$

https://doi.org/10.1017/S0022377806004533 Published online by Cambridge University Press

augmented by Ohm's law derived from magnetohydrodynamic (MHD) equations

$$\mathbf{j}_\perp = \frac{\Sigma_A}{V_A}\partial_t \mathbf{E}_\perp, \quad j_z = \sigma_\parallel E_z,$$

where $\Sigma_A = c^2/(4\pi V_A)$ is the Alfvén wave conductance.

In this system the possible MHD disturbances are described by the following equations for Alfvén waves, carrying the field-aligned current j_z, and fast compressional waves, carrying the field-aligned magnetic field disturbance B_z,

$$\begin{aligned} \partial_{tt} j_z - V_A^2 \partial_{zz} j_z &= \frac{c^2}{4\pi}\nabla_\perp^2 \partial_t(\sigma_\parallel^{-1} j_z), \\ \partial_{tt} B_z - V_A^2 \nabla^2 B_z &= 0. \end{aligned} \tag{2.1}$$

These equations are decoupled. This means that the excitation of Alfvén-type disturbances is not accompanied by a generation of a compressional mode. This mode coupling in homogeneous plasma can take place if a transverse (Hall) conductivity is non-vanishing ($\sigma_\perp \neq 0$).

We assume that the ARL is a thin layer as compared with the Alfvén wavelength. Therefore, the thin-layer approximation can be used, that is, the ARL thickness $b \to 0$, whereas its resistivity $Q(x, y, t) = b/\sigma_\parallel$ remains finite.

In this approximation the simple Alfvén wave equation is valid in the upper ($z > 0$) and lower ($z < 0$) hemi-spaces

$$\partial_{tt} j_z - V_A^2 \partial_{zz} j_z = 0. \tag{2.2}$$

This equation must be supplemented with two boundary conditions at the interface $z = 0$ between two hemi-spaces, separated by a thin layer ($b \to 0$) with the resistivity Q. The first condition is the requirement of the continuity of field-aligned current $j_z(x, y, z, t)$ across the ARL, which enables us to consider the function $j_z^{(0)}(x, y, t) = j_z(x, y, 0, t)$ (the superscript (0) indicates that current is considered inside the ARL). The second boundary condition is obtained by integration of the first equation from the system (2.1) across the layer and subsequent transition to the limit $b \to 0$, as follows

$$\{\partial_z j_z\}_{z=0} + \nabla_\perp^2 \partial_t [R(x, y, t) j_z^{(0)}] = 0. \tag{2.3}$$

Here

$$R(x, y, t) = \frac{c^2}{4\pi V_A^2} Q = \Sigma_A Q V_A^{-1}$$

is the normalized resistance of the ARL, and $\{\partial_z j_z\}_{z=0} = \partial_z j_z(x, y, +0, t) - \partial_z j_z(x, y, -0, t)$ is the jump of the current density derivative across the ARL.

3. Self-consistent model of the Alfvén front interaction with the ARL

From the magnetosphere, a front of field-aligned current transported by an Alfvén wave impinges the topside ionosphere along the z-axis:

$$j_z = j_0(x, y, z, t) = J(z - z_0(x, y) + V_A t). \tag{3.1}$$

A function $J(z)$ is assumed to be monotonically growing; then this Alfvén wave front produces a gradual increase of the field-aligned current density in the layer at $z = 0$. As soon as the current density $j_z^{(0)}$ exceeds a threshold value j_*, an

https://doi.org/10.1017/S0022377806004533 Published online by Cambridge University Press

anomalous field-aligned resistance ignites. This process will be described by the very simplified two-step model [14]

$$R(j_z^{(0)}) = \begin{cases} 0 & \text{if } j_z^{(0)} < j_*, \\ R_0 & \text{if } j_z^{(0)} > j_*. \end{cases} \tag{3.2}$$

Thus, we consider the self-consistent problem, that is, we take into account that the ARL resistance depends on the magnitude of current inside the layer.

We suppose that the monotonic function $J(z)$ is such that $J(0) = j_*$. Then the wave 'critical' front, that is, the surface where $j_0(x, y, z, t) = j_*$, is $z = z_0(x, y) - V_A t$. Let us suppose that the critical front at $t = 0$ intersects with the plane $z = 0$ at a point $x = 0, y = 0$, whereas the function $z_0(x, y)$ is monotonically growing along the rays $x = \rho\cos\phi$, $y = \rho\sin\phi$, $\rho > 0$ with the growth of ρ (ρ and ϕ are coordinates in a local cylindrical coordinate system centered at the point of first 'encounter' of the Alfvén front with a layer).

Below the critical front ($z < z_0(x, y) - V_A t$) the solution of (2.2), (2.3), where $R(x, y, t)$ is given by (3.2), is the undisturbed wave (3.1). The region $D_{AR}(t)$ in the plane $z = 0$, where anomalous resistivity has been switched-on, $R(x, y, t) \neq 0$, is bounded by the curve $z_0(x, y) = V_A t$; within the region $D_{AR}(t)$ an inequality $z_0(x, y) < V_A t$ takes place.

The disturbance caused by the turn-on of anomalous resistance propagates from the plane $z = 0$. The source of this disturbance is the region growing with time $D_{AR}(t)$. The solution of (2.2) for $t \geqslant 0$ evidently has the form

$$j_z(x, y, z, t) = \begin{cases} J(z - z_0(x, y) + V_A t) + j_{zA}(x, y, t - z/V_A), & z \geq 0; \\ J(z - z_0(x, y) + V_A t) + j_{zA}(x, y, t + z/V_A), & z \leq 0. \end{cases} \tag{3.3}$$

This solution for the whole space is determined by the function $j_{zA}(x, y, t)$, defined at the border $z = 0$. This function characterizes the induced field-aligned current density, transported by the induced Alfvén impulse.

The second boundary condition (2.3) enables us to obtain an equation to determine the induced field-aligned current density $j_{zA}(x, y, t)$ and the total density of the current through the layer at $z = 0$:

$$j_z^{(0)} = J(-z_0(x, y) + V_A t) + j_{zA}(x, y, t). \tag{3.4}$$

Substituting the jump of the current density derivative across the ARL found from (3.3), that is, $\{\partial_z j_z\}_{z=0} = -2V_A^{-1}\partial_t j_{zA}$, into the condition (2.3), one obtains the following equation

$$\partial_t\left[-2j_{zA}(x, y, t) + V_A\nabla_\perp^2\left(Rj_z^{(0)}\right)\right] = 0. \tag{3.5}$$

Thus, the expression in square brackets does not vary in time. This invariant value is zero at any point of the plane $z = 0$, because before the arrival of the critical front ($t < 0$) throughout this plane $j_{zA} \equiv 0$ and $R \equiv 0$ (actually j_{zA} and R are vanishing even before the moment $t = V_A^{-1} z_0(x, y)$). As a result, from (3.5) taking into account (3.4), one can obtain the equation

$$V_A\nabla_\perp^2(Rj_z^{(0)}) - 2j_z^{(0)} = -2J_0, \tag{3.6}$$

where $J_0(x, y, t) = J(V_A t - z_0(x, y))$ is the given density of the external current in the plane $z = 0$. If we solve (3.6), with the use of (3.4) we may find the function $j_{zA}(x, y, t)$ and calculate by formula (3.3) the solution of (2.2), (2.3) throughout the

https://doi.org/10.1017/S0022377806004533 Published online by Cambridge University Press

entire space at any time moment. Note that the differential equation (3.6) holds the time t just as a parameter.

It is more convenient to consider (3.6) as an equation with respect to the variable $Rj_z^{(0)}$, which is proportional to the potential drop across the layer ($\varphi_\parallel = \lim_{b\to 0} E_z b$):

$$Rj_z^{(0)} = \Sigma_{\rm A} V_{\rm A}^{-1} Q \sigma_\parallel E_z = \Sigma_{\rm A} V_{\rm A}^{-1} \varphi_\parallel$$

($Q = b/\sigma_\parallel$ for $b \to 0$). For an easy comparison with relevant relationships from [11] and [12] we use as a searched function the Alfvén potential at the upper boundary of the ARL, that is, $\varphi = \varphi(x, y, +0, t)$. This function is related to $\varphi_\parallel$ by the relationship $\varphi_\parallel = -2\varphi$. Therefore, (3.6) is reduced to the following form

$$\Sigma_{\rm A} \nabla_\perp^2 \varphi + j_z^{(0)} = J_0. \tag{3.7}$$

Here the current density $j_z^{(0)}$ is to be considered as a function of φ, which in accordance with (3.2) has the form

$$j_z^{(0)}(\varphi) = \begin{cases} j_* \left(\dfrac{\varphi}{\varphi_*} \right) & \text{if } \varphi \le \varphi_*, \\ j_* & \text{if } \varphi_* \le \varphi < 0, \end{cases} \tag{3.8}$$

where

$$\varphi_* = -\tfrac{1}{2} \Sigma_{\rm A}^{-1} V_{\rm A} R_0 j_* = -\tfrac{1}{2} Q_0 j_*. \tag{3.9}$$

The occurrence of permanent value of current $j_z^{(0)}(\varphi) = j_*$ upon potential drop across the ARL less than some critical value corresponds physically to the plasma state near the instability threshold. In this state the resistance R has some intermediate value between zero and R_0. In fact, (3.7) is the modification of (17) from [11] or (10) from [12]. However, in contrast with the above papers, here the dependence $j_z^{(0)}(\varphi)$ is nonlinear. The potential $\varphi(x, y)$ is proportional to the tangential to the cylindrical boundary of the anomalous resistivity region component of electric field E_z (before the transfer to the thin layer limit $b \to 0$). Therefore, $\varphi(x, y)$ is to be continuous upon the transition across the boundary $J_0(x, y) = j_*$, that is, the curve $z_0(x, y) = V_{\rm A} t$. Beyond the region $D_{\rm AR}$, the function $\varphi(x, y) \equiv 0$. Thus, the boundary condition for (3.7) is

$$\varphi(x, y) = 0 \quad \text{at the boundary of } D_{\rm AR}.$$

The field-aligned current density $j_z^{(0)}(x, y)$ is also a continuous function in the entire plane $z = 0$, because $j_z^{(0)}$ depends on the potential φ continuously according to the expression (3.8).

4. One-dimensional case

Let us consider the case when the external front (3.1) does not depend on y coordinate. In this case, (3.7) has the form

$$\varphi'' = \Sigma_{\rm A}^{-1} [J_0(x, t) - j_z^{(0)}(\varphi)], \tag{4.1}$$

where $J_0(x, t) = J(V_{\rm A} t - z_0(x))$. It is an ordinary differential equation, since it contains the time t as a parameter. The searched solution of (4.1) must be such that $\varphi(x_-) = \varphi(x_+) = 0$, where $x_\pm(t)$ are roots of the equation $J_0(x, t) = j_*$. The region

https://doi.org/10.1017/S0022377806004533 Published online by Cambridge University Press

$D_{\rm AR}$ is reduced to the interval $x_- < x < x_+$. The solution is searched within the interval (x_-, x_+); beyond this interval $\varphi(x) \equiv 0$.

If the integral curve of (4.1), connecting $(x_-, 0)$ and $(x_+, 0)$ does not go down below the level $\varphi = \varphi_*$, then with regard for (3.8) it can be described by a simple equation

$$\varphi'' = \Sigma_{\rm A}^{-1} \Delta_0(x,t), \tag{4.2}$$

where $\Delta_0(x,t) = J_0(x,t) - j_*$ is the surpass of the external current above the threshold. Its solution under the condition $\varphi(x_-) = \varphi(x_+) = 0$ is

$$\varphi(x) = k_-(x - x_-) + \Sigma_{\rm A}^{-1} \int_{x_-}^{x} d\xi \int_{x_-}^{\xi} \Delta_0(\eta)\, d\eta, \tag{4.3}$$

where the slope at $x = x_-$ is determined by

$$k_- = -\frac{1}{\Sigma_{\rm A}(x_+ - x_-)} \int_{x_-}^{x_+} d\xi \int_{x_-}^{\xi} \Delta_0(\eta)\, d\eta.$$

The formula (4.3) is relevant to the initial stage of the process, because the expansion of the region $D_{\rm AR} = (x_-, x_+)$ and growth of the external current above the threshold reduce the minimum of the function (4.3). After the minimum reaches the level φ_*, the integral curve $\varphi = \varphi(x)$ in its middle part gets to the region $\varphi < \varphi_*$, where owing to (3.8) it is determined by the linear equation

$$\varphi'' = \lambda_{\rm A}^{-2} \varphi + \Sigma_{\rm A}^{-1} J_0(x,t), \tag{4.4}$$

where the linear scale $\lambda_{\rm A} = \sqrt{V_{\rm A} R_0/2} = \sqrt{\Sigma_{\rm A} Q_0/2}$ is related to the field-aligned resistivity. The parameter $\lambda_{\rm A}$ named the Alfvén damping scale was introduced in [15,16]. Note also the relation $\varphi_* = -\lambda_{\rm A}^2 j_*/\Sigma_{\rm A}$ following from (3.9). The solution of (4.4) can be expressed analytically via quadratures. The complete solution is to be obtained by the smooth merging of the solutions of (4.2) and (4.4). At the initial phase (while $\min \varphi(x) > \varphi_*$) the current density $j_z^{(0)}$ remains at the threshold level j_* throughout the whole region $D_{\rm AR}$.

5. Examples of external current fronts

5.1. Step-wise plane front

As a simple example, we consider a step-wise spatial distribution of the external current density in (4.2):

$$J_0(x,t) = J_0(t)\eta(\Lambda_\perp - |x|),$$

where $\eta(x)$ is the Heaviside function ($\eta(x < 0) = 0$ and $\eta(x \geq 0) = 1$). Let the variation of $J_0(t)$ have a typical time scale T_0. The external current front (3.1) with $z_0(x) = 0$ is assumed to be flat inside a limited region $|x| < \Lambda_\perp$, beyond this region the current vanishes. Thus, the area $D_{\rm AR}$ is the interval $(-\Lambda_\perp, \Lambda_\perp)$.

First, we consider the simpler case when the solution $\varphi(x)$ does not go down below the value φ_*. The solution of (4.2) with the conditions $\varphi(-\Lambda_\perp) = \varphi(\Lambda_\perp) = 0$ is

$$\varphi(x) = \tfrac{1}{2}\varphi_* \lambda_{\rm A}^{-2} [j_*^{-1} J_0(t) - 1](\Lambda_\perp^2 - x^2). \tag{5.1}$$

When the external current increases linearly in time, that is, $J_0(t) = j_*(1 + t/T_0)$, the value

$$|\min \varphi(x)| = \tfrac{1}{2}\varphi_* (\Lambda_\perp/\lambda_{\rm A})^2 (t/T_0) \tag{5.2}$$

https://doi.org/10.1017/S0022377806004533 Published online by Cambridge University Press

also grows linearly in time. The minimum of $\varphi(x)$ reaches the level φ_*, when $(\Lambda_\perp/\lambda_\mathrm{A})^2(t/T_0) = 2$. Thus, the current $j_z^{(0)}$ remains at the threshold level j_* during the retardation time

$$T_\mathrm{d} = 2T_0\left(\frac{\lambda_\mathrm{A}}{\Lambda_\perp}\right)^2.$$

In the general case, this delay time T_d can be determined as a root of the equation

$$J_0(T_\mathrm{d}) = j_*[1 + 2(\lambda_\mathrm{A}/\Lambda_\perp)^2]. \tag{5.3}$$

If the current density $J_0(t)$ never exceeds the value of $j_*[1 + 2(\lambda_\mathrm{A}/\Lambda_\perp)^2]$, then the value of potential $\varphi(x)$ does not go below φ_*, whereas $j_z^{(0)}$ remains at the threshold level while $J_0(t) \geq j_*$.

At $t > T_\mathrm{d}$, the minimum of $\varphi(x)$ goes below φ_*. The region $-x_* < x < x_*$ arises, where the solution is determined by (4.4), and beyond this region (4.2) is still valid. Integrating (4.2) and (4.4) with the account of the boundary conditions $\varphi(\pm\Lambda_\perp) = 0$ and $\varphi(\pm x_*) = \varphi_*$ we find

$$\varphi(x,t) = \begin{cases} \varphi_1(x,t) & \text{at } x_* \leq x \leq \Lambda_\perp, \\ \varphi_2(x,t) & \text{at } |x| \leq x_*, \\ \varphi_1(-x,t) & \text{at } -\Lambda_\perp \leq x \leq -x_*, \end{cases}$$

where the functions φ_1 and φ_2 are determined by

$$\frac{\varphi_1(x,t)}{\varphi_*} = \frac{\Lambda_\perp - x}{\Lambda_\perp - x_*} + \frac{1}{2\lambda_\mathrm{A}^2}[j_*^{-1}J_0(t) - 1](\Lambda_\perp - x)(x - x_*)$$

and

$$\frac{\varphi_2(x,t)}{\varphi_*} = 1 + \left[\frac{J_0(t)}{j_*} - 1\right]\left[1 - \frac{\cosh(x/\lambda_\mathrm{A})}{\cosh(x_*/\lambda_\mathrm{A})}\right].$$

To find the joining point x_*, we use the condition

$$\partial_x\varphi_1(x_*,t) = \partial_x\varphi_2(x_*,t).$$

In the example under consideration, this condition is, in fact, the following equation

$$\frac{1}{1-\xi_*} - [j_*^{-1}J_0(t) - 1]\left[\frac{1}{2}\frac{\Lambda_\perp^2}{\lambda_\mathrm{A}^2}(1-\xi_*) + \frac{\Lambda_\perp}{\lambda_\mathrm{A}}\tanh\left(\frac{\Lambda_\perp}{\lambda_\mathrm{A}}\xi_*\right)\right] = 0, \tag{5.4}$$

where $\xi_* = x_*/\Lambda_\perp$. This equation implicitly determines the dependence $x_*(t)$. At $t > T_\mathrm{d}$, (5.4) has a root in the interval $0 < \xi_* < 1$.

Linear growth of an external current $J_0(t) = j_*(1 + t/T_0)$ corresponds to a general situation during an initial phase after the threshold has been exceeded. Numerically calculated time evolution of main parameters under linear growth of $J_0(t)$ is shown in Figs 2–4.

Figure 2 shows the time evolution of the normalized potential as a set of curves $\varphi(x,t)/\varphi_*$ at equal intervals $\Delta\tau = 0.04$ of dimensionless time $\tau = t/T_0$. At the initial phase the anomalous resistivity grows corresponding to the jump at $j_z^{(0)} = j_*$ of the function (3.2). The fast potential growth at this stage is specific for a 'wide' external current front with $\Lambda_\perp/\lambda_\mathrm{A} \gg 1$, as is seen from (5.2). Later, at the phase with constant $R(j_z^{(0)}) = R_0$, the potential increases much slower.

https://doi.org/10.1017/S0022377806004533 Published online by Cambridge University Press

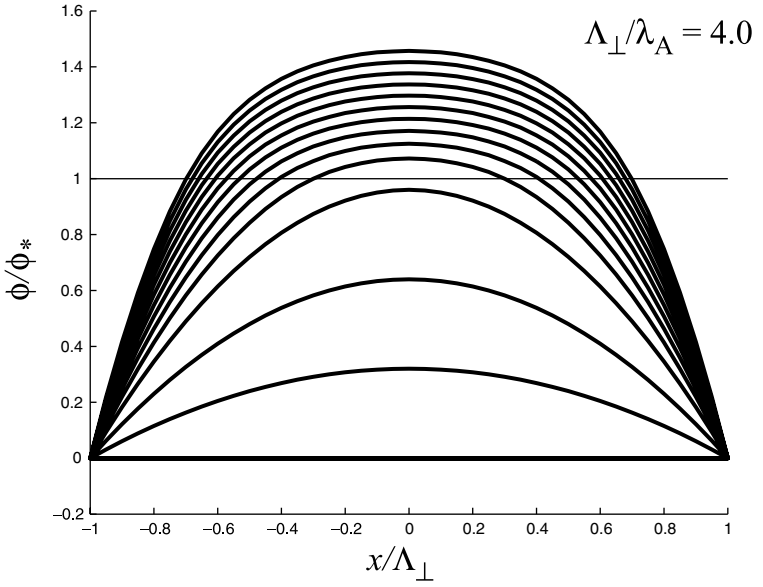

Figure 2. The time evolution of the potential as a set of curves $\varphi_*^{-1}\varphi(x,t)$ at equal intervals $\Delta\tau = 0.04$ of dimensionless time $\tau = t/T_0$.

The time evolution of φ at the center of ARL $x = 0$ is explicitly shown in Fig. 3(a). The fast growth of $\varphi(t)$ during time interval T_d is replaced by slower increase, after $\varphi(t)$ has reached the level φ_*.

The time evolution of $j_z^{(0)}/j_* - 1$ during linear phase of the external current growth is shown in Fig. 3(b). When the current has reached the level j_*, it remains on this level for the time T_d, and only continues to grow after this. The nominal growth of external current $J_0/j_* - 1$ in the absence of ARL is indicated by dotted line. In these figures the parameter $\Lambda_\perp/\lambda_\mathrm{A} = 4.0$.

The time evolution of the induced field-aligned current density $j_{z\mathrm{A}}$ at the ARL center $x = 0$ is shown in Fig. 4 for several values of the parameter $\Lambda_\perp/\lambda_\mathrm{A}$, indicated near curves. This current induced during the transition from one plasma state to another (within ARL) initially increases in absolute value totally compensating for any further increase of an external current. However, after some time (T_d) the induced current cannot compensate for the growth of external current.

Now we consider the interaction with ARL of a field-aligned current front that grows in time and then saturates at some level. This time behavior can be modeled by the dependence $J_0(t) = j_*[1 + \tanh(t/T_0)]$. The time evolution of the induced current density $j_{z\mathrm{A}}(0,t)$ for several values of the parameter $\Lambda_\perp/\lambda_\mathrm{A}$ calculated for this model is shown in Fig. 5, analogous to Fig. 4. At smaller values of $\Lambda_\perp/\lambda_\mathrm{A}$ the time evolution of $j_{z\mathrm{A}}(0,t)$ under saturated current differs from that under linearly growing external current. Figure 6 presents the corresponding set of the curves $j_z^{(0)}(t) - j_*$ together with the applied external current $\Delta_0 = J_0 - j_*$ (dotted line). Once again, as in Fig. 3(b), one can see that the current through the ARL is delayed for some time at the critical level j_*, and only then continue to grow.

The saturation level of the external current $J_0(t)$ with this time dependence is $J_0(\infty) = 2j_*$. If this value does not exceed $j_*[1 + 2(\lambda_\mathrm{A}/\Lambda_\perp)^2]$ (see (5.3)), then for relatively narrow current fronts $\Lambda_\perp/\lambda_\mathrm{A} \le \sqrt{2}$ the total current $j_z^{(0)}(x,t)$ is retarded

https://doi.org/10.1017/S0022377806004533 Published online by Cambridge University Press

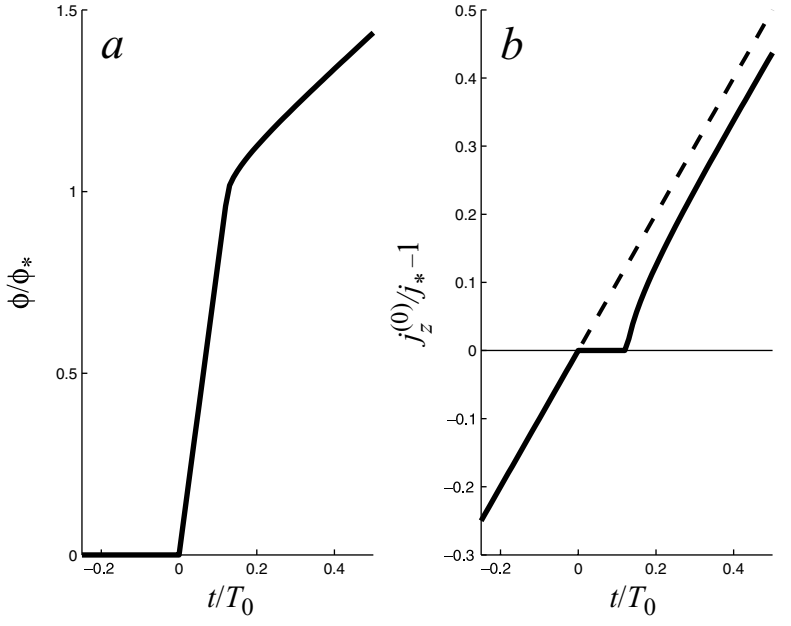

Figure 3. (a) The time evolution of φ at the fixed point $x = 0$. (b) The same for $j_z^{(0)}/j_* - 1$. The nominal growth of external current $J_0/j_* - 1$ in the absence of ARL is indicated by a dotted line. The parameter $\Lambda_\perp/\lambda_\mathrm{A} = 4.0$.

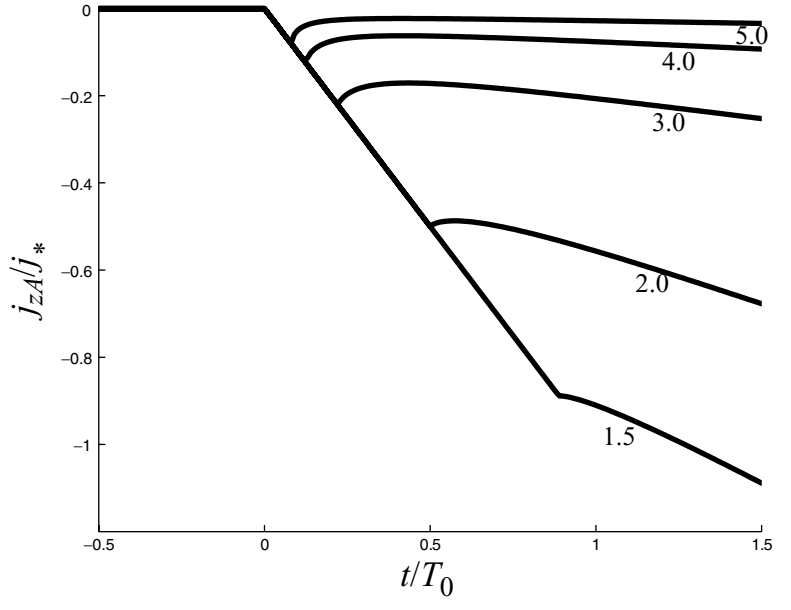

Figure 4. The time evolution of the induced field-aligned current density $j_{z\mathrm{A}}$ at the fixed point $x = 0$ for several values of the parameter $\Lambda_\perp/\lambda_\mathrm{A}$, indicated near curves. The model of linearly growing external current.

https://doi.org/10.1017/S0022377806004533 Published online by Cambridge University Press

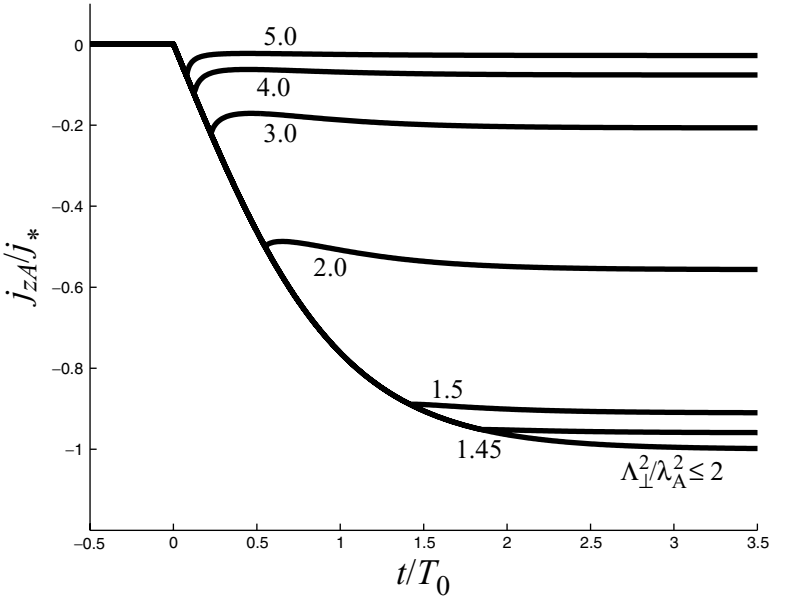

Figure 5. The time evolution of the induced current density $j_{z\mathrm{A}}(0,t)$ for several values of the parameter $\Lambda_\perp/\lambda_\mathrm{A}$ for the model of external current with saturation at some level.

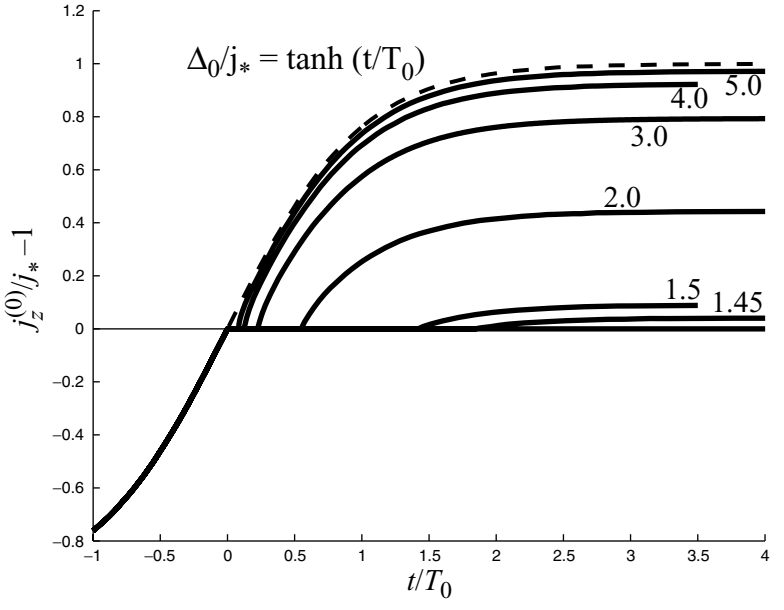

Figure 6. The set of the curves $j_z^{(0)}(t)/j_* - 1$ (solid curves) together with the external current $J_0/j_* - 1$ (dashed curve). The values $\Lambda_\perp/\lambda_\mathrm{A}$ are indicated near corresponding curves.

https://doi.org/10.1017/S0022377806004533 Published online by Cambridge University Press

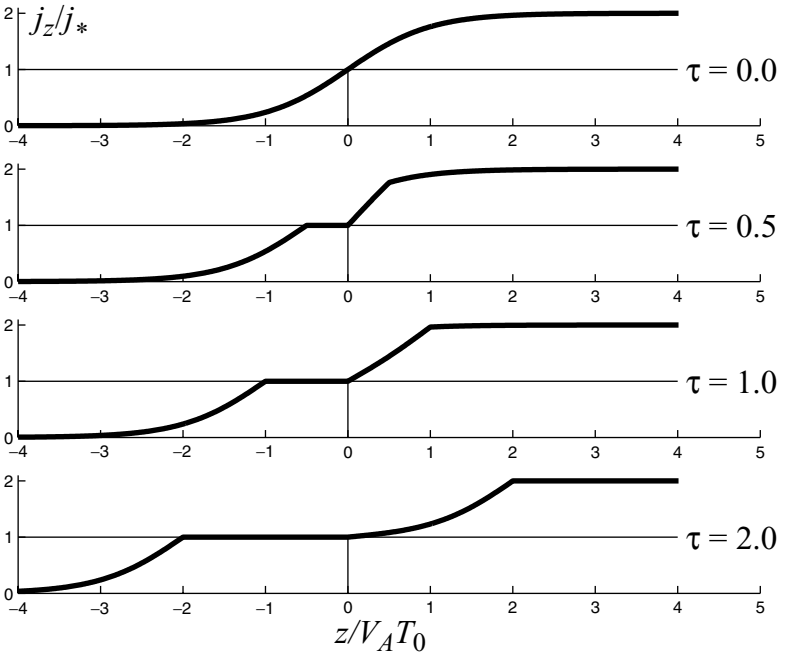

Figure 7. The time evolution of spatial field-aligned structure of Alfvén impulse at the background of an external current front for the case of 'narrow' ARL ($\Lambda_\perp/\lambda_A \leq \sqrt{2}$). The 'snapshots' of the field-aligned structure $j_z(z)$ are shown for several subsequent time moments in the middle of the ARL ($x = 0$).

at the threshold level j_* for an indefinitely long time, that is, $T_d = \infty$. If the current front is relatively wide, $\Lambda_\perp/\lambda_A > \sqrt{2}$, then the total current is delayed for a finite time T_d at the threshold level, and then $\max_x j_z^{(0)}(x,t)$ continues to grow. For these two cases, Fig. 7 ($\Lambda_\perp/\lambda_A \leq \sqrt{2}$) and Fig. 8 ($\Lambda_\perp/\lambda_A = 2.0$) show the time evolution of spatial field-aligned structure of Alfvén impulse at the background of external current front, described by the dependence (3.3). The 'snapshots' of the field-aligned structure $j_z(z)$ are shown for several subsequent time moments in the middle of the ARL ($x = 0$). The ARL location corresponds to $z = 0$. One can see that in the case of a 'narrow layer' (Fig. 7), the ARL works as a 'current limiter' that does not allow a current with density higher than a critical level j_* to flow through the ARL.

However, in the case of a 'wide layer' (Fig. 8), the ARL just hampers the growth of the external current for some time at a critical level, but then the current through the ARL continues to increase. The changes of spatial scales in the range $\Lambda_\perp/\lambda_A \leq \sqrt{2}$ do not influence the resultant spatial–temporal pattern of induced disturbance.

5.2. Parabolic front

This example can be considered as a model of a general situation at an early stage, when only the leading terms in the Taylor decomposition of the functions $z_0(x)$ and $J(z)$ are kept. Let us consider the situation when external current linearly grows, and the critical front has a parabolic shape

$$z_0(x) = ax^2 = L_\parallel x^2/L_\perp^2,$$
$$J(z) = j_* + bz = j_*(z/L_\parallel + 1),$$

https://doi.org/10.1017/S0022377806004533 Published online by Cambridge University Press

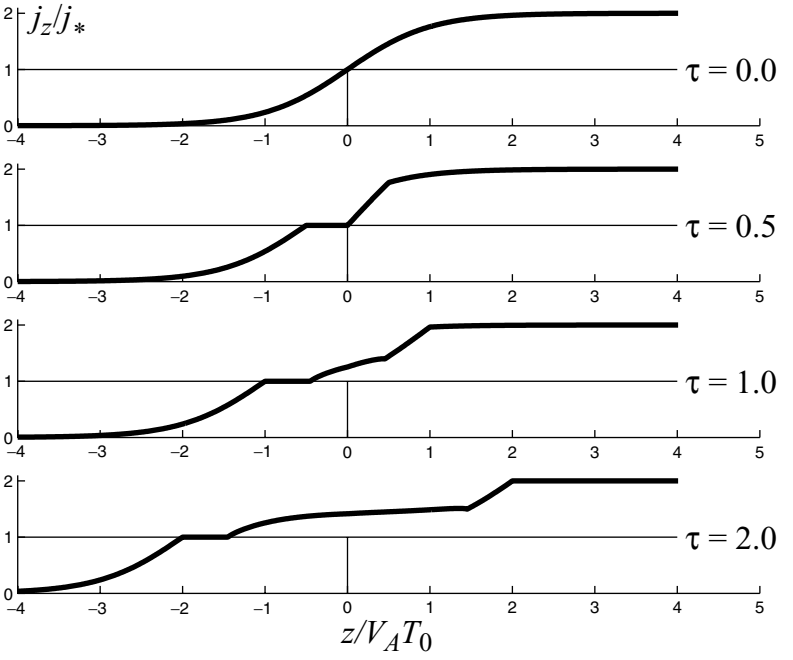

Figure 8. The time evolution of spatial field-aligned structure of Alfvén impulse at the background of external current front for the case of 'wide' ARL (parameters ratio $\Lambda_\perp/\lambda_A = 2.0$ taken as an example). The 'snapshots' of the field-aligned structure $j_z(z)$ are shown for several subsequent time moments in the middle of the ARL ($x = 0$).

where $L_\parallel = V_A T_0$ and $L_\perp$ are longitudinal and transverse scales of the external current front. Then

$$\Delta_0(x,t) = b(V_A t - ax^2) = j_*(t/T_0 - x^2/L_\perp^2). \tag{5.5}$$

The region D_{AR} is bounded by points $x_\pm = \pm L_\perp\sqrt{t/T_0}$. The principal distinction of this example from the previous one is that here the region D_{AR} first occurs at a point, but then its size grows in time.

At the initial stage, while $\varphi(x) \geq \varphi_*$, the potential is determined by (4.2) with Δ_0 from (5.5). Its solution with the conditions $\varphi(x_-) = \varphi(x_+) = 0$ may be presented as

$$\varphi(x) = \frac{1}{12}\varphi_*\left(\frac{L_\perp t}{\lambda_A T_0}\right)^2\left[5 - 6\left(\frac{x}{x_+}0\right)^2 + \left(\frac{x}{x_+}\right)^4\right]. \tag{5.6}$$

This shows that $|\min\varphi(x)|$ grows as the square of time. The form of dependence $\varphi(x)$ is universal and is determined by the polynomial $\frac{1}{12}(5 - 6\xi^2 + \xi^4)$, where $\xi = x/x_+(t)$, and $|\xi| \leq 1$. The minimum of $\varphi(x)$ reaches the level φ_*, when $L_\perp t/\lambda_A T_0 = \sqrt{12/5}$. Thus, the current $j_z^{(0)}$ remains at the threshold level j_* during the time

$$T_d = \sqrt{\frac{12}{5}}T_0\frac{\lambda_A}{L_\perp}.$$

At $t > T_d$ the region $-x_* < x < x_*$ arises, where the solution is determined by (4.4), and beyond this region (4.2) is still valid. Using the conditions $\varphi(x_\pm) = 0$ and

https://doi.org/10.1017/S0022377806004533 Published online by Cambridge University Press

$\varphi(\pm x_*) = \varphi_*$ we obtain the solution, which has the form

$$\varphi(x,t) = \begin{cases} \varphi_1(x,t) & \text{at } x_* \le x \le x_+, \\ \varphi_2(x,t) & \text{at } |x| \le x_*, \\ \varphi_1(-x,t) & \text{at } x_- \le x \le -x_*, \end{cases} \tag{5.7}$$

where the functions φ_1 and φ_2 are determined by

$$\frac{\varphi_1(x,t)}{\varphi_*} = \frac{x_+ - x}{x_+ - x_*} + \frac{(x_+ - x)(x - x_*)}{12\lambda_A^2 L_\perp^2}[5x_+^2 - (x + x_*)(x_+ + x_*) - x^2]$$

and

$$\frac{\varphi_2(x,t)}{\varphi_*} = 1 + \frac{1}{L_\perp^2}\left[x_+^2 - x^2 - 2\lambda_A^2 - (x_+^2 - x_*^2 - 2\lambda_A^2)\frac{\cosh(x/\lambda_A)}{\cosh(x_*/\lambda_A)}\right].$$

To find the joining point x_* we use the smoothness condition, which for our given example looks as follows (for $\xi_* = x_*/x_+$)

$$\frac{1}{1-\xi_*} - \left(\frac{L_\perp t}{\lambda_A T_0}\right)^2 P(\xi_*) - \sqrt{\frac{t}{T_0}}\left[\frac{L_\perp t}{\lambda_A T_0}(1-\xi_*^2) - 2\frac{\lambda_A}{L_\perp}\right]\tanh\left(\sqrt{\frac{t}{T_0}}\frac{L_\perp}{\lambda_A}\xi_*\right)$$

$$- 2\frac{t}{T_0}\xi_* = 0, \tag{5.8}$$

where the polynomial $P(\xi_*) = \frac{1}{12}(5 - 7\xi_* - \xi_*^2 + 3\xi_*^3)$. If $L_\perp t/(\lambda_A T_0) > \sqrt{12/5} = 1.5492$, that is, at $t > T_d$, (5.8) has a root in the interval $0 < \xi_* < 1$.

Calculations with the help of relations (5.7), (3.8) and (3.4) provide results similar to the plane front case. The time evolution of φ for a parabolic front (not shown) is similar to that shown in Fig. 3(a). The difference is that the fast growth of $|\varphi(x,t)|$ occurs not only in time, but expands fast from the ARL center, and the time dependence is not linear (e.g. square of time at $x = 0$). The time evolutions of $j_z^{(0)}$ and induced current j_{zA} are also similar to those shown in Fig. 3(b) and Fig. 4, correspondingly.

Figures 9(a) and (b) present several successive 'snapshots' of the evolution of the transverse spatial structure of the field-aligned current $j_z^{(0)}(x)$ with the plane and parabolic front, respectively, at various stages of the anomalous resistance occurrence. In both cases, after retardation time T_d the current $j_z^{(0)}$ exceeds the critical value in a spatially limited 'tongue', that grows in magnitude and expands in space in the transverse direction.

6. Discussion: consequences of the model

The primary application of this model is the excitation of a transient magnetic pulse during the auroral activity activation in the terrestrial magnetosphere. It is commonly assumed that the acceleration of precipitating electrons necessary for auroral activation is produced by an anomalous field-aligned electric field. The analytical consideration of the anomalous resistivity onset in this paper has shown that during the entrance of field-aligned current front into the ARL, the Alfvénic impulse is generated. Therefore, the occurrence of such an impulse signifies the 'switch-on' of the anomalous resistivity on auroral field lines and thus may be an indicator of the transition of a global magnetospheric instability into the phase with ionospheric feedback. The occurrence of resonant features of the ionosphere–magnetosphere

https://doi.org/10.1017/S0022377806004533 Published online by Cambridge University Press

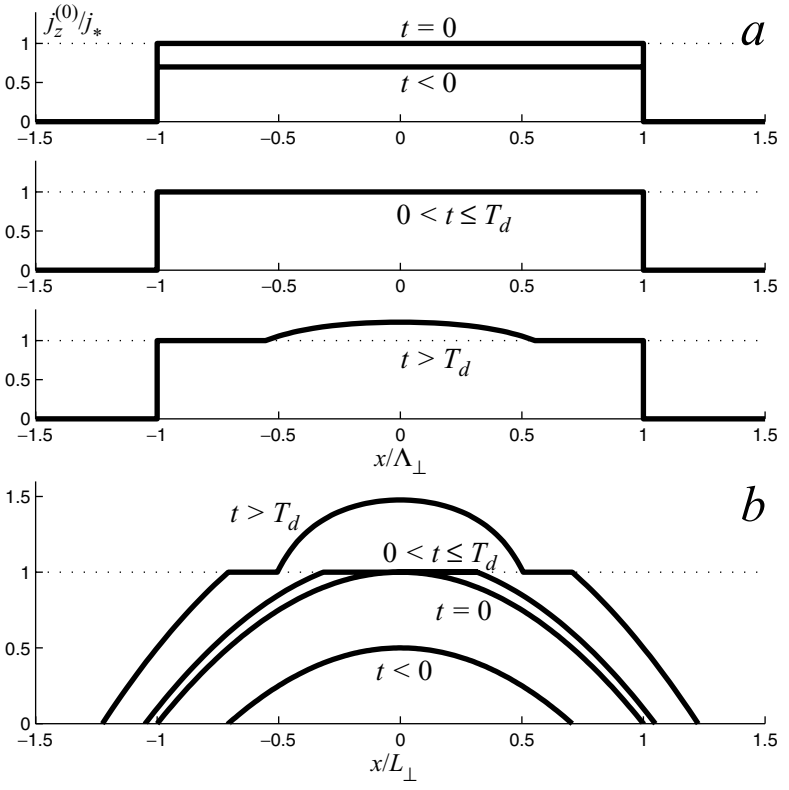

Figure 9. The evolution of the transverse spatial structure of the field-aligned current $j_z^{(0)}(x)$ for a model with the (a) plane and (b) parabolic front of the external current at various stages of the anomalous resistance occurrence.

system can produce oscillatory transient response. This mechanism can contribute to the generation of transient impulsive signals at auroral latitudes, classified as Pi2 pulsations. Indeed, a general association within a few minutes between the Pi2 wave train and the substorm onset, auroral breakup, onset of geomagnetic bay and explosive phenomena in the nightside terrestrial magnetosphere (current disruption, dipolarization, X-line formation, bursty bulk flows, etc.) is well established [17–19]. At auroral latitudes, Pi2 transient disturbances probably, in fact, comprise inputs from several possible driver mechanisms, and a 'classical' Pi2 waveform, isolated damping quasi-sinusoidal train, is commonly observed at middle latitudes [20]. Because of multiple possible nearly simultaneous contributions to Pi2 pulsations, still there is no confirmative physical interpretation of their generation mechanism. The fine temporal structure of auroral Pi2 may be used as a clue to the understanding and monitoring of a substorm explosive phase. Recently, the dedicated analysis of the magnetic array data indeed revealed the contributions from several sources into the auroral Pi2 signals [21, 22]. We suppose that such an additional transient Pi2-like signal is generated during the sudden occurrence of ARL during substorm onset on auroral field lines, as was originally suggested by Arykov and Maltsev [11].

The interaction of current with ARL results in the delay of the current growth through the layer by the time about T_d. Calculations show that the delay time T_d

https://doi.org/10.1017/S0022377806004533 Published online by Cambridge University Press

as compared with the nominal growth time of the external current $T_0 = L_\parallel / V_\mathrm{A}$ is as follows

$$\frac{T_\mathrm{d}}{T_0} \simeq \frac{\lambda_\mathrm{A}}{L_\perp}.$$

Therefore, an ARL operates as a kind of 'current limitation device' that does not allow an external current to exceed a critical level. Depending on the ratio between the Alfvén damping scale λ_A and external current width $L_\perp$, the retardation time T_d may vary in a wide range (up to infinity!).

A number of plasma effects have been neglected in our consideration. The occurrence of anomalous resistance is to be accompanied by the plasma heating and formation of pressure gradients. However, we assume that the process of the Alfvén front interaction with ARL considered here is faster than a heating process. Then, in a weakly turbulent plasma, nonlinear wave interaction provides a nonlinear frequency shift, namely $\omega_k^2 \to \omega_k^2 + \delta_k^2$. The modification of dispersion relationship calculated by Aleksin et al. [23] is by order of magnitude $\delta^2/\omega^2 \sim (k_\perp/k_\parallel)^2 (W/B^2)^{2/3}$, where W is the energy density of turbulent pulsations. However, the neglected effects cannot noticeably modify the results obtained.

7. Conclusion

Our analysis has shown that the onset of anomalous resistance in a current-carrying plasma is to be accompanied by MHD effects. These MHD effects can result in the generation of kink Alfvénic disturbance and termination of the external current growth. The magnitude of the effect is dependent on the ratio between the transverse scale of the external current and specific parameter of the ARL, the Alfvén resistive scale λ_A. The retardation of the external current growth is important for a 'wide' anomalous resistivity domain ($\Lambda_\perp \gg \lambda_\mathrm{A}$), whereas a 'narrow' anomalous resistivity domain ($L_\perp \ll \lambda_\mathrm{A}$) does not exert a significant influence on the external current.

Acknowledgements

This research is supported by the RFBR grant 04-05-64321 (NM, AL) and INTAS grant 03-05-5359 (EF, VP).

References

[1] Kadomzev, B. B. 1964 Plasma turbulence. *Rev. Plasma Phys.* **4**, 188–339.

[2] Galeev, A. A. and Sagdeev, R. Z. 1973 Nonlinear plasma theory. *Rev. Plasma Phys.* **7**, 3–145.

[3] Fredricks, R. W., Scarf, F. L. and Russell, C. T. 1973 Field-aligned currents, plasma waves, and anomalous resistivity in the disturbed polar cusp. *J. Geophys. Res.* **78**, 2133–2141.

[4] Lysak, R. L. 1990 Electrodynamic coupling of the magnetosphere and ionosphere. *Space Sci. Rev.* **52**, 33–87.

[5] Gudkova, V. A., Barsukov, V. M., Zeleny, L. M., Volosevich, A. V., Loginov, G. A. and Liperovsky, V. A. 1974 Turbulence in magnetospheric plasma and damping of Pi2 variations. *Geomagn. Aeronomy* **14**, 764–766.

[6] Liperovsky, V. A. and Pudovkin, M. I. 1983 *Anomalous Resistivity and Double Layers in the Magnetospheric Plasma*. Moscow: Nauka, p. 181 (in Russian).

[7] Trakhtenhertz, V. Yu. and Feldstein, A. Ya. 1985 About dissipation of Alfvén waves in the layer with anomalous resistance. *Geomag. Aeronomy* **25**, 334–336.

[8] Tikhonchuk, V. T. and Bychenkov, V. Y. 1995 Effect of anomalous resistivity on MHD wave damping. *J. Geophys. Res.* **100**, 9535–9538.

[9] Lysak, R. L. 1991 Feedback instability of the ionospheric resonant cavity. *J. Geophys. Res.* **96**, 1553–1568.

[10] Pokhotelov, O. A., Khruschev, V., Parrot, M., Senchenkov, S. and Pavlenko, V. P. 2001 Ionospheric Alfvén resonator revisited: Feedback instability. *J. Geophys. Res.* **106**, 25 813–25 824.

[11] Arykov, A. A. and Maltsev, Yu. P. 1983 Generation of Alfvén waves in an anomalous resistivity region. *Planet. Space Sci.* **31**, 267–273.

[12] Pilipenko, V., Mazur, N., Fedorov, E., Uozumi, T. and Yumoto, K. 2005 Excitation of Alfvén impulse by the anomalous resistance onset on the auroral field lines. *Ann. Geophys.* **23**, 1455–1465.

[13] Kindel, J. M. and Kennel, C. F. 1971 Topside current instabilities. *J. Geophys. Res.* **76**, 3055–3078.

[14] Streltsov, A. V. and Lotko, W. 2003 Reflection and absorption of Alfvénic power in the low-altitude magnetosphere. *J. Geophys. Res.* **108**, 8016, doi:10.1029/2002JA009425.

[15] Vogt, J. 2002 Alfvén wave coupling in the auroral current circuit. *Surveys Geophys.* **23**, 335–377.

[16] Fedorov, E., Pilipenko, V. and Engebretson, M. J. 2001 ULF wave damping in the auroral acceleration region. *J. Geophys. Res.* **106**, 6203–6212.

[17] Liou, K., Meng, C.-I., Newell, P. T., Takahashi, K., Ohtani, S.-I., Lui, A. T. Y., Brittnacher, M. and Parks, G. 2000 Evaluation of low-latitude Pi2 pulsations as indicators of substorm onset using Polar ultraviolet imagery. *J. Geophys. Res.* **105**, 2495–2505.

[18] Shiokawa, K., et al. 1998 High-speed ion flow, substorm current wedge, and multiple Pi2 pulsations. *J. Geophys. Res.* **103**, 4491–4508.

[19] Kepko, L., Kivelson, M. G. and Yumoto, K. 2001 Flow bursts, braking, and Pi2 pulsations. *J. Geophys. Res.* **106**, 1903–1915.

[20] Olson, J. V. 1999 Pi2 pulsations and substorm onsets: A review. *J. Geophys. Res.* **104**, 17 499–17 520.

[21] Uozumi, T., Yumoto, K., Kawano, H., Yoshikawa, A., Olson, J. V., Solovyev, S. I. and Vershinin, E. F. 2000 Characteristics of energy transfer of Pi 2 magnetic pulsations: Latitudinal dependence. *Geophys. Res. Lett.* **27**, 1619–1622.

[22] Kohta, H., Yoshikawa, A. and Yumoto, K. 2005 Wave characteristics of Pi2 pulsations observated at the CPMN stations: Results from the independent component analysis. In *Proc. of the Chapman Conf. on Magnetospheric ULF Waves, San Diego, CA, American Geophysical Union, Washington*, p. 21 025.

[23] Aleksin, V. F., Makarenko, V. N., Pavitsky, P. D. and Khodusov, V. D. 1989 Modified Alfvén wave dispersion law in the weakly turbulent plasma with anisotropic pressure. *Ukrainian Phys. J.* **34**, 1712–1715 (in Russian).